Molecular Plant Pathology

MOLECULAR PLANT PATHOLOGY (2017) 18(3), 347–362 DOI: 10.1111/mpp.12401

Rhamnose synthase activity is required for pathogenicity of the vascular wilt fungus *Verticillium dahliae*

PARTHASARATHY SANTHANAM[1], JORDI C. BOSHOVEN[1,†], OMAR SALAS[2,†], KYLE BOWLER[2,†], MD TOHIDUL ISLAM[1], MOJTABA KEYKHA SABER[1], GRARDY C. M. VAN DEN BERG[1], MAOR BAR-PELED[2] AND BART P. H. J. THOMMA[1,*]

[1]*Laboratory of Phytopathology, Wageningen University, Droevendaalsesteeg 1, 6708 PB, Wageningen, the Netherlands*
[2]*Complex Carbohydrate Research Center, University of Georgia, Athens, GA 30602, USA*

SUMMARY

The initial interaction of a pathogenic fungus with its host is complex and involves numerous metabolic pathways and regulatory proteins. Considerable attention has been devoted to proteins that play a crucial role in these interactions, with an emphasis on so-called effector molecules that are secreted by the invading microbe to establish the symbiosis. However, the contribution of other types of molecules, such as glycans, is less well appreciated. Here, we present a random genetic screen that enabled us to identify 58 novel candidate genes that are involved in the pathogenic potential of the fungal pathogen *Verticillium dahliae*, which causes vascular wilt diseases in over 200 dicotyledonous plant species, including economically important crops. One of the candidate genes that was identified concerns a putative biosynthetic gene involved in nucleotide sugar precursor formation, as it encodes a putative nucleotide-rhamnose synthase/epimerase-reductase (NRS/ER). This enzyme has homology to bacterial enzymes involved in the biosynthesis of the nucleotide sugar deoxy-thymidine diphosphate (dTDP)-rhamnose, a precursor of L-rhamnose, which has been shown to be required for virulence in several human pathogenic bacteria. Rhamnose is known to be a minor cell wall glycan in fungi and has therefore not been suspected as a crucial molecule in fungal–host interactions. Nevertheless, our study shows that deletion of the VdNRS/ER gene from the *V. dahliae* genome results in complete loss of pathogenicity on tomato and *Nicotiana benthamiana* plants, whereas vegetative growth and sporulation are not affected. We demonstrate that VdNRS/ER is a functional enzyme in the biosynthesis of uridine diphosphate (UDP)-rhamnose, and further analysis has revealed that *VdNRS/ER* deletion strains are impaired in the colonization of tomato roots. Collectively, our results demonstrate that rhamnose, although only a minor cell wall component, is essential for the pathogenicity of *V. dahliae*.

Keywords: *Agrobacterium tumefaciens*-mediated transformation (ATMT), attachment, carbohydrate, root colonization, tomato, UDP-rhamnose, vascular wilt.

* *Correspondence*: Email: bart.thomma@wur.nl
†These authors contributed equally to this work.

INTRODUCTION

Vascular wilt diseases caused by soil-borne pathogens are amongst the most devastating plant diseases worldwide. The fungus *Verticillium dahliae* causes vascular wilt diseases in over 200 dicotyledonous plant species, including important crops, such as eggplant, lettuce, olive, spinach and tomato (Fradin and Thomma, 2006; Klosterman *et al.*, 2009). Triggered by root exudates, the melanized resting structures, microsclerotia, germinate and penetrate the roots through the root tips, wounds or sites of lateral root formation (Fradin and Thomma, 2006). After crossing the cortex, the hyphae of the fungus grow into the xylem vessels. The mycelium remains exclusively in these vessels and produces conidia which are transported acropetally with the water flow in the xylem throughout the plant. On senescence, microsclerotia are produced that are released into the soil on tissue decomposition (Wilhelm, 1955). Typical symptoms of plants infected with *V. dahliae* comprise stunting, wilting, chlorosis and vascular browning (Pegg and Brady, 2002).

Verticillium wilt diseases are difficult to control because of the longevity of the microsclerotia and the inability of fungicides to eliminate the fungus once it has entered the xylem tissues of the host plant (Fradin and Thomma, 2006; Wilhelm, 1955). Moreover, crop rotation is ineffective because of the broad host range of *V. dahliae*. The only effective control measure, soil fumigation, is expensive and has harmful environmental effects (Rowe *et al.*, 1987). As a consequence, genetic resistance is presently preferred to control *Verticillium* wilt diseases. Importantly, *Verticillium* resistance has been described in several plant species, including crops (Bolek *et al.*, 2005; Hayes *et al.*, 2011; Schaible *et al.*, 1951; Simko *et al.*, 2004). From tomato (*Solanum lycopersicum*), the *Ve1 Verticillium* resistance gene has been cloned that mediates resistance to race 1 strains of *V. dahliae* that express the secreted Ave1 effector (Fradin *et al.*, 2009; de Jonge *et al.*, 2012). Putative *Ve1* orthologues have been identified within and outside the Solanaceae family, suggesting that *Ve1*-mediated *Verticillium* resistance may be widespread in plants (Thomma *et al.*, 2011). Interestingly, Ave1 contributes to *V. dahliae* virulence on susceptible tomato plants, and homologues occur in a handful of taxonomically unrelated plant-pathogenic fungi (de Jonge *et al.*, 2012).

Various other virulence genes have been identified in *V. dahliae*, including members of the expanded LysM effector and NEP-like (NLP) protein family (de Jonge *et al.*, 2013; Klimes *et al.*, 2015; Klosterman *et al.*, 2011; Santhanam *et al.*, 2013). Furthermore, genome analysis has revealed the relative abundance of particular families of cell wall-degrading enzymes (CWDEs) when compared with other fungi (Klosterman *et al.*, 2011). The importance of CWDEs during pathogenicity was demonstrated by the disruption of the CWDE regulator VdSNF1, which reduced *V. dahliae* virulence (Tzima *et al.*, 2011). In addition, genes involved in nitrogen and amino acid metabolism were found to be important for establishment in the nutrient-poor vascular system (Singh *et al.*, 2010; Timpner *et al.*, 2013). Finally, virulence genes have been described that are also involved in stress tolerance (Klimes *et al.*, 2015).

The identification and subsequent characterization of novel genes involved in disease establishment are of fundamental importance to understand the interaction between *V. dahliae* and its hosts, and to potentially design novel strategies for disease control. An effective way to identify novel pathogenicity genes in plant-pathogenic fungi is the use of random mutagenesis coupled with a rapid technique to screen the mutants for phenotypes. *Agrobacterium tumefaciens* is a Gram-negative soil bacterium that can infect hosts as diverse as fungi, oomycetes and plants, and can be used to randomly insert a transfer DNA (T-DNA) into the host genome. Over recent years, *A. tumefaciens*-mediated transformation (ATMT) has been used to identify genes involved in disease development in various plant pathogens (Giesbert *et al.*, 2012; Hüser *et al.*, 2009; Jeon *et al.*, 2007; Korn *et al.*, 2015; Maruthachalam *et al.*, 2011; Michielse *et al.*, 2009; Munch *et al.*, 2011; Ramos *et al.*, 2013; Schumacher *et al.*, 2014; Xu and Chen, 2013). In this study, we report the identification of pathogenicity and virulence genes in *V. dahliae* through ATMT. A collection of 900 transformants of *V. dahliae* was generated and tested for reduced disease development on susceptible tomato plants. We subsequently studied one of the candidates in detail, a gene that putatively encodes a biosynthetic gene involved in nucleotide sugar precursor formation, to reveal its role in pathogenicity.

RESULTS

Identification of random *V. dahliae* transformants affected in aggressiveness

In this study, we generated 900 random T-DNA insertion mutants of *V. dahliae* by transforming conidiospores through ATMT. All transformants were assessed for reduced potential to cause disease on tomato seedlings by root-dip inoculation and scored for typical disease symptoms, including stunting, wilting, chlorosis and necrosis, for up to 14 days post-inoculation (dpi). Seedlings that exhibited reduced *Verticillium* wilt symptoms when compared with plants inoculated with wild-type *V. dahliae* were selected, and the corresponding *V. dahliae* mutants were retained for rescreening, leading to a set of 200 transformants. Subsequently, after calibration of the conidial concentration in the inoculum to 10^6 conidia/mL, all 200 transformants were reassessed for compromised ability to cause wilt disease on tomato plants for up to 21 dpi. Eventually, 80 transformants showed a reproducible defect in disease development when compared with the wild-type progenitor strain (Fig. 1).

Isolation of T-DNA flanking regions in selected *V. dahliae* transformants

Inverse polymerase chain reaction (iPCR) was carried out on the 80 selected transformants to determine the T-DNA insertion sites. The genomic borders flanking the T-DNA were amplified, sequenced and the resulting sequences were queried against the *V. dahliae* genome (Faino *et al.*, 2015). In this manner, sequences flanking the T-DNA were determined for 65 mutants, whereas T-DNA flanking regions repeatedly could not be amplified from any of the borders of the remaining 15 mutants. Of the 65 flanking sequences, 12 sequences corresponded to the backbone of the vector that was used for ATMT, whereas 10 sequences could not unambiguously be assigned to a single genomic location. The remaining 43 sequences resulted in single genomic hits, allowing the determination of T-DNA integration sites. In total, 14 insertions were found within predicted open reading frames (ORFs; Table 1), of which two transformants carried an insertion in the same ORF, whereas the remaining 29 insertions occurred in non-coding regions. For these 29 insertions, the predicted genes flanking the T-DNA were identified. In one case, we found that, for two transformants, the T-DNA was integrated into the same non-coding region, albeit at a slightly different location, resulting in the identification of the same flanking genes. In another case, the same candidate gene was identified twice in two transformants as a result of an insertion upstream and downstream of the gene. One flanking gene was only identified at 55,077 bp from the insertion site, for which we disqualified it as a candidate gene. In total, this resulted in the identification of 55 candidate genes from the 29 mutants with insertions in non-coding regions.

In order to try to determine which of the two genes flanking a particular insertion site in the non-coding region is likely to cause reduced disease development, *in planta* expression of the flanking genes was assessed making use of previously generated RNAseq data of *V. dahliae*-inoculated *Nicotiana benthamiana* plants (Faino *et al.*, 2012; de Jonge *et al.*, 2012). For 10 insertions, this revealed that only one of the two flanking genes is expressed during infection, disqualifying the 10 candidate genes that are not expressed. Thus, 45 candidate genes were considered from mutants with an insertion in the non-coding region and 13 candidate genes were identified from mutants with an insertion in the ORF (Table 1).

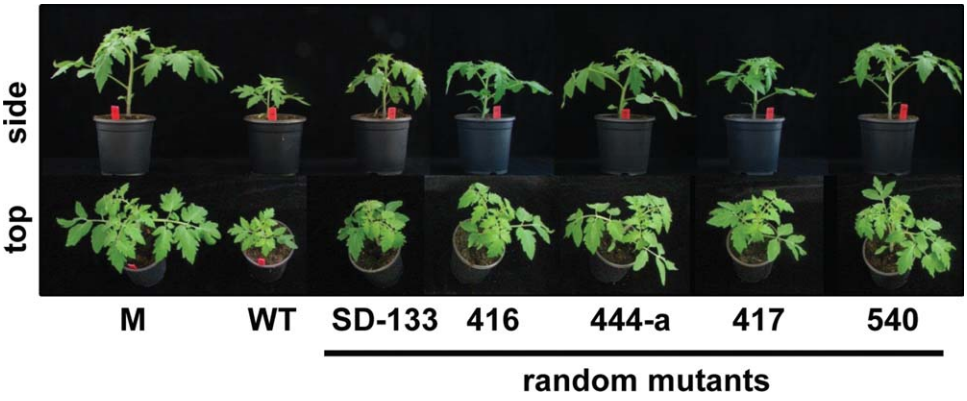

Fig. 1 Typical assay to identify transformants with reduced pathogenicity or virulence. Ten-day-old tomato seedlings were mock inoculated (M) or inoculated with conidiospores of wild-type *Verticillium dahliae* (WT) or random T-DNA insertion mutants. At 21 days post-inoculation, the plants were scored for disease development by comparing plants inoculated with wild-type *V. dahliae* with those inoculated with the T-DNA insertion mutants. The sides (top) and tops (bottom) of plants inoculated with five T-DNA insertion mutants that are impaired in aggressiveness are shown.

Subsequently, the 58 candidate genes were queried against the pathogen–host interaction (PHI) database that contains experimentally verified pathogenicity and virulence factors of plant and animal pathogens (Winnenburg *et al.*, 2006, 2008); this resulted in the identification of homologues ($E < 10^{-6}$) for only 19 of the 58 candidate genes (Table 2).

Analysis of a T-DNA insertion site links *VdNRS/ER* to virulence

In random mutant 389, the T-DNA was integrated 56 bp upstream of the coding sequence (CDS) of a nucleotide-rhamnose synthase/epimerase-reductase (NRS/ER) homologue VDAG_06010 (Table 1; Klosterman *et al.*, 2011), which corresponds to VDAG_JR2_Chr7g02960 in the *V. dahliae* JR2 assembly deposited at http://fungi.ensembl.org/ (Faino *et al.*, 2015). The first CDS downstream of the T-DNA insertion site is found only at 2.4 kb, encoding a squalene synthetase (VDAG_06011 or VDAG_JR2_Chr7g02950), an enzyme that has been implicated in sterol and triterpene biosynthesis. However, considering the distance between the T-DNA insertion and the CDS of this gene, it is unlikely that it is affected and causal to the reduced pathogenicity phenotype of the RM-389 mutant. To assess whether any genes had been overlooked by the automated gene prediction in the region between the T-DNA insertion and the squalene synthetase CDS, RNAseq reads from *V. dahliae*-inoculated *N. benthamiana* (Faino *et al.*, 2012; de Jonge *et al.*, 2012) were queried. However, no reads were found to map to this region, suggesting that no *in planta* transcribed genes reside in this region. Finally, with real-time PCR on genomic DNA, using the single copy *Ave1* gene as a reference (de Jonge *et al.*, 2012), it was determined that only a single T-DNA insertion was present in the genome of the RM-389 mutant.

Verticillium dahliae NRS/ER (VdNRS/ER) shows weak (17%) amino acid sequence similarity to the *Salmonella enterica* deoxythymidine diphosphate (dTDP)-rhamnose biosynthesis component rmlD, a bacterial protein involved in the last step in the conversion of dTDP-glucose to dTDP-rhamnose. In bacteria, the nucleotide sugar dTDP-rhamnose is the precursor that facilitates the incorporation of L-rhamnose into glycan, which has been implicated in the virulence of pathogenic bacteria such as *Salmonella enterica*, *Vibrio cholerae* and *Streptococcus mutans* (Giraud *et al.*, 2000). Thus, considering all of the above, functional analysis of the *VdNRS/ER* gene was pursued.

VdNRS/ER is required for *V. dahliae* pathogenicity

Assessment of *VdNRS/ER* expression on various growth media (potato dextrose broth, Czapek-Dox, Murashige and Skoog medium) revealed that the gene is expressed under these conditions (data not shown). Targeted replacement of *VdNRS/ER* by a hygromycin resistance cassette through homologous recombination was pursued in wild-type *V. dahliae*. Several independent *VdNRS/ER* deletion strains were obtained, two of which (*Δ6010-1* and *Δ6010-2*) were used for further analysis (Fig. S1, see Supporting Information). To assess the role of *VdNRS/ER* in *V. dahliae* vegetative growth and conidiospore production, radial growth and sporulation of the *VdNRS/ER* deletion strains on potato dextrose agar were assessed, together with the random mutant (RM-389) and an ectopic transformant with a random T-DNA insertion outside of the *VdNRS/ER* gene. This analysis showed that growth and conidiation were not markedly affected on *VdNRS/ER* deletion (Fig. 2).

Subsequently, the role of *VdNRS/ER* in *V. dahliae* pathogenicity was addressed. To this end, the expression of *VdNRS/ER* was assessed in wild-type *V. dahliae* during infection of tomato plants

Table 1 List of candidate genes identified based on the T-DNA insertion sites in the random mutants that showed compromised virulence on tomato.

T-DNA insertion within the CDS

Mutant	Old locus†	New locus‡	Annotation	Expression§	CDS¶
78	Not available	VDAG_JR2_Chr1g08240	Glycoside hydrolase	+	–
73	Not available	VDAG_JR2_Chr1g08240	Glycoside hydrolase	+	–
407	VDAG_00500	VDAG_JR2_Chr1g19180	Carboxypeptidase D	+	–
659	VDAG_02200	VDAG_JR2_Chr2g03300	α/β-Hydrolase fold family	–	–
SD-133	VDAG_04418	VDAG_JR2_Chr3g02140	Ran GTPase-activating protein 1	+	–
444-B	VDAG_08830	VDAG_JR2_Chr3g07650	Acetate kinase	+	–
211	VDAG_06985	VDAG_JR2_Chr4g06020	Leucine-rich repeat protein	+	–
375	VDAG_07314	VDAG_JR2_Chr4g10770	Copper amine oxidase 1	+	–
416	VDAG_10292	VDAG_JR2_Chr5g06230	Conserved hypothetical protein	–	–
174	VDAG_05684	VDAG_JR2_Chr5g09640	Hypothetical protein	+	–
657-2	VDAG_04769	VDAG_JR2_Chr6g09500	Phospho-2-dehydro-3-deoxyheptonate aldolase	+	–
367	VDAG_06253	VDAG_JR2_Chr7g00300	Cyclic nucleotide-binding protein	+	–
618	VDAG_08151	VDAG_JR2_Chr8g01560	Hypothetical protein	+	–
48	VDAG_08150	VDAG_JR2_Chr8g01570	CaiB/BaiF family enzyme	–	–

T-DNA insertion in intergenic region

	Upstream direction						Downstream direction					
Mutant	Dist.*	Old locus†	New locus‡	Annotation	Expression§	CDS¶	Dist.†	Old locus	New locus‡	Annotation	Expression§	CDS¶
459-1	2485	VDAG_00838	VDAG_JR2_Chr1g01770	Predicted protein	+	–	1784	VDAG_00839	VDAG_JR2_Chr1g01780	Transcription initiation factor TFIID subunit 12	+	–
143	374	VDAG_00843	VDAG_JR2_Chr1g01820	Not annotated	+	–	100	VDAG_00844	VDAG_JR2_Chr1g01830	Exosome complex exonuclease	+	–
SD-102	270	VDAG_00599	VDAG_JR2_Chr1g20260	Histidinol-phosphate aminotransferase	+	–	746	VDAG_00600	VDAG_JR2_Chr1g20270	Acetyl esterase	+	–
44	545	VDAG_08030	VDAG_JR2_Chr1g22770	Deuterolysin metalloprotease	–	–	669	VDAG_08031	VDAG_JR2_Chr1g22760	SAFF domain containing protein	+	–
11	100	VDAG_08003	VDAG_JR2_Chr1g23050	F-box protein	–	–	3330	VDAG_08988	VDAG_JR2_Chr1g23040	UMTA methyltransferase	+	–
SD-107	165	VDAG_07796	VDAG_JR2_Chr1g25310	Hydrolase	+	–	1586	VDAG_07797	VDAG_JR2_Chr1g25300	Briggsae CBR-SMU-2 protein	+	–
182	470	VDAG_09439	VDAG_JR2_Chr2g01480	SMC N-terminal-containing protein	+	–	257	VDAG_09440	VDAG_JR2_Chr2g01470	SGT1-like protein	+	–
525	895	VDAG_02343	VDAG_JR2_Chr2g01760	Cell wall glucanase	+	100	71	VDAG_02344	VDAG_JR2_Chr2g01750	Phosphoribosylglycinamide formyltransferase	+	–
SD-7	215	VDAG_02014	VDAG_JR2_Chr2g05250	Myb-like DNA-binding protein	+	–	1004	VDAG_02015	VDAG_JR2_Chr2g05240	Zinc NFX1-type-containing protein	–	–
540	622	VDAG_01960	VDAG_JR2_Chr2g05800	KH domain containing protein	+	–	336	VDAG_01961	VDAG_JR2_Chr2g05790	DUF974 protein	+	–
402	1788	VDAG_01891	VDAG_JR2_Chr2g06520	Domain-containing protein	+	400	1318	VDAG_01892	VDAG_JR2_Chr2g06510	Hypothetical protein	+	100
417	88	VDAG_01651	VDAG_JR2_Chr2g09280	F-box protein	+	–	731	VDAG_01652	VDAG_JR2_Chr2g09270	Cytochrome p450 protein	–	–
622	700	Not available	VDAG_JR2_Chr3g02050	Unknown	+	–	101	VDAG_04427	VDAG_JR2_Chr3g02040	AGC/AKT protein kinase	+	–
SD-89	335	VDAG_07703	VDAG_JR2_Chr4g00600	Transcriptional regulatory protein pro-1	–	–	423	VDAG_07704	VDAG_JR2_Chr4g00580	Pathway-specific nitrogen regulator	+	–

Table 1 *Continued*

T-DNA insertion in intergenic region												
	Upstream direction						Downstream direction					
Mutant	Dist.*	Old locus†	New locus‡	Annotation	Expression§	CDS¶	Dist.†	Old locus	New locus‡	Annotation	Expression§	CDS¶
SD-78	1214	VDAG_07011	VDAG_JR2_Chr4g05750	Subunit of Golgi mannosyltransferase complex	+	–	1914	VDAG_07012	VDAG_JR2_Chr4g05740	Fungal-specific transcription factor	+	–
414	4	Not available	VDAG_JR2_Chr4g08330	Myomesin	–	–	1466	Not available	VDAG_JR2_Chr4g08340	UMTA methyltransferase	–	–
584	51	VDAG_09007	VDAG_JR2_Chr4g08540	Family protein	+	–	1221	VDAG_09008	VDAG_JR2_Chr4g08550	Zinc-binding dehydrogenase	+	–
534	737	VDAG_09007	VDAG_JR2_Chr4g08540	Family protein	+	–	535	VDAG_09008	VDAG_JR2_Chr4g08550	Zinc-binding dehydrogenase	+	–
199	64	VDAG_05141	VDAG_JR2_Chr5g01900	Low-affinity potassium transport protein	–	–	703	VDAG_05142	VDAG_JR2_Chr5g01910	Sodium ion/H ion antiporter	+	–
412	1647	VDAG_09301	VDAG_JR2_Chr5g03950	Potassium sodium efflux p-type fungal type	+	–	1459	VDAG_09302	VDAG_JR2_Chr5g03940	Glycoside hydrolase family 43 protein	+	100
550	78	VDAG_04591	VDAG_JR2_Chr6g07500	Calmodulin	+	–	667	VDAG_04592	VDAG_JR2_Chr6g07510	AP-1 complex subunit γ-1	+	–
SD-94	716	VDAG_04810	VDAG_JR2_Chr6g09950	NADPH dehydrogenase	+	–	1014	VDAG_04811	VDAG_JR2_Chr6g09960	Hypothetical protein	–	100
75	1060	VDAG_09054	VDAG_JR2_Chr6g10940	Ubiquitin fusion degradation protein	+	–	196	VDAG_09055	VDAG_JR2_Chr6g10930	Ubiquitin fusion degradation protein	+	–
374	1023	VDAG_06275	VDAG_JR2_Chr7g00090	Maintenance of telomere capping 1	+	–	279	VDAG_06276	VDAG_JR2_Chr7g00080	Major facilitator superfamily transporter	+	–
389	56	VDAG_06010	VDAG_JR2_Chr7g02960	NAD-dependent epimerase dehydratase	+	–	2363	VDAG_06011	VDAG_JR2_Chr7g02950	Squalene synthetase	+	–
438	977	VDAG_10534	VDAG_JR2_Chr7g06650	CTP synthase	+	–	55077	VDAG_06595	VDAG_JR2_Chr7g06640	SAD1/UNC protein	+	–
59	47	VDAG_10192	VDAG_JR2_Chr7g10460	Benzoate 4-monooxygenase cytochrome P450	–	–	1565	VDAG_10193	VDAG_JR2_Chr7g10450	Cellulose-binding family II	+	–
646	246	VDAG_10191	VDAG_JR2_Chr7g10470	Methyltransferase	+	–	422	VDAG_10192	VDAG_JR2_Chr7g10460	Benzoate 4-monooxygenase cytochrome p450	–	–
575	466	VDAG_03431	VDAG_JR2_Chr8g09910	Vegetative cell wall protein gp1-like	–	–	1040	VDAG_03432	VDAG_JR2_Chr8g09920	DUF221 protein	+	–

*Distance from the T-DNA to the coding sequence (CDS).

†Locus corresponds to the *Verticillium dahliae* strain VdLs.17 assembly deposited at http://genome.jgi.doe.gov/programs/fungi/ (Klosterman *et al*., 2011).

‡Locus corresponds to the *Verticillium dahliae* strain JR2 assembly deposited at http://fungi.ensembl.org/ (Faino *et al*., 2015).

§Evidence for *in planta* expression.

¶Evidence for expression in the region between T-DNA and the closest open reading frame (ORF). Distances from T-DNA are indicated in base pairs (bp).

Table 2 Homologues identified in the pathogen–host interaction (PHI) database among the 58 potential *Verticillium dahliae* pathogenicity genes.

Old locus*	New locus†	Annotation	E-value	Accession‡
VDAG_00839	VDAG_JR2_Chr1g01780	Transcription initiation factor tfiid subunit 12	7E-19	PHI:2168
VDAG_00844	VDAG_JR2_Chr1g01830	Exosome complex exonuclease	5E-12	PHI:3472
VDAG_01461	VDAG_JR2_Chr1g08260	Ring finger protein	2E-09	PHI:1393
VDAG_00500	VDAG_JR2_Chr1g19180	Carboxypeptidase D	4E-55	PHI:901
VDAG_09440	VDAG_JR2_Chr2g01470	SGT-1-like protein	1E-156	PHI:1615
VDAG_09439	VDAG_JR2_Chr2g01480	SMC N-terminal-containing protein	2E-10	PHI:359
VDAG_02343	VDAG_JR2_Chr2g01760	Cell wall glucanase	9E-30	PHI:816
VDAG_02014	VDAG_JR2_Chr2g05250	Myb-like DNA-binding protein	1E-105	PHI:1540
VDAG_01960	VDAG_JR2_Chr2g05800	KH domain containing protein	3E-22	PHI:1662
VDAG_04427	VDAG_JR2_Chr3g02040	AGC/AKT protein kinase	0E+00	PHI:3131
VDAG_07704	VDAG_JR2_Chr4g00580	Pathway-specific nitrogen regulator	0E+00	PHI:1960
VDAG_07012	VDAG_JR2_Chr4g05740	Fungal-specific transcription factor	0E+00	PHI:1954
VDAG_09008	VDAG_JR2_Chr4g08550	Zinc-binding dehydrogenase	7E-13	PHI:2895
VDAG_07314	VDAG_JR2_Chr4g10770	Copper amine oxidase 1	1E-106	PHI:2171
VDAG_09301	VDAG_JR2_Chr5g03950	Potassium sodium efflux p-type fungal type	0E+00	PHI:2098
VDAG_04591	VDAG_JR2_Chr6g07500	Calmodulin	4E-20	PHI:2640
VDAG_06253	VDAG_JR2_Chr7g00300	Cyclic nucleotide-binding protein	2E-10	PHI:372
VDAG_10193	VDAG_JR2_Chr7g10450	Cellulose-binding family II	6E-13	PHI:2388
VDAG_10191	VDAG_JR2_Chr7g10470	Methyltransferase	9E-40	PHI:2315

*Locus corresponds to the *V. dahliae* strain VdLs.17 assembly deposited at http://genome.jgi.doe.gov/programs/fungi/ (Klosterman *et al.*, 2011).
†Locus corresponds to the *V. dahliae* strain JR2 assembly deposited at http://fungi.ensembl.org/ (Faino *et al.*, 2015).
‡PHI database accession.

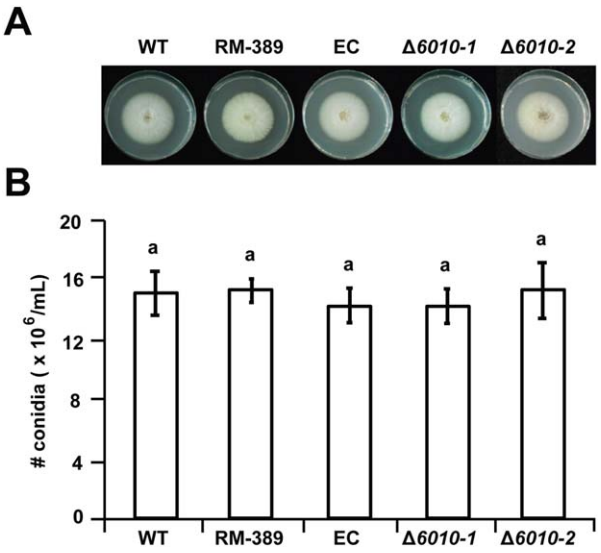

Fig. 2 Targeted deletion of *VdNRS/ER* (NRS/ER, nucleotide-rhamnose synthase/epimerase-reductase) does not impair growth and conidiogenesis. (A) Radial growth and colony morphology of wild-type *Verticillium dahliae* (WT), random transformant RM-389, an ectopic transformant (EC) and two *VdNRS/ER* deletion strains (Δ*6010-1* and Δ*6010-2*) after 7 days of incubation on potato dextrose agar (PDA) medium at 22°C. (B) Average number of conidia produced after 7 days of growth on PDA medium based on two independent experiments. Letters indicate significant differences ($P < 0.05$) calculated using Student's *t*-test.

in a time course harvested at regular intervals after inoculation, showing that *VdNRS/ER* is induced during *in planta* growth with a peak in expression at around 12 dpi (Fig. 3). Subsequently, the *VdNRS/ER* deletion strains were inoculated on tomato plants, alongside the random mutant (RM-389) and an ectopic transformant, to investigate the role of *VdNRS/ER* in fungal virulence. Although inoculation of the plants with the wild-type *V. dahliae* strain and the ectopic transformant resulted in the development of symptoms of *Verticillium* wilt disease that included stunting of the plants and wilting, inoculation with RM-398 or the *VdNRS/ER* deletion strains did not result in disease development (Fig. 4A). The absence of disease symptoms was confirmed by measuring the surface area of the foliage of the plants that were inoculated with the various fungal strains. Plants that were inoculated with *VdNRS/ER* deletion strains developed similar foliage (canopy) areas to mock-inoculated plants and plants inoculated with RM-389 (Fig. 5A). In contrast, less foliage developed in plants that were inoculated with the wild-type *V. dahliae* strain and the ectopic transformant (Fig. 5A). Thus, we conclude that *VdNRS/ER* is crucial for disease development by *V. dahliae*. To assess whether *VdNRS/ER* deletion strains retained the capability to colonize tomato plants, fungal outgrowth assays were performed by plating of stem sections harvested from the hypocotyls of the inoculated plants. Interestingly, although the ectopic transformants and the wild-type strain extensively colonized the stems of tomato plants, no outgrowth was observed for the *VdNRS/ER* deletion strains and RM-389, demonstrating that these genotypes were not able to colonize the xylem vessels of the inoculated tomato

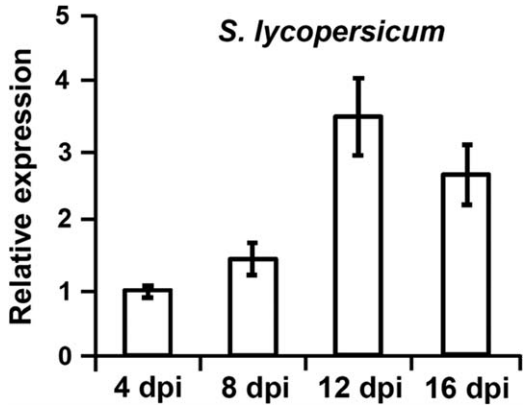

Fig. 3 Expression of *VdNRS/ER* (NRS/ER, nucleotide-rhamnose synthase/epimerase-reductase) during infection of *Verticillium dahliae* on tomato. Ten-day-old tomato (*Solanum lycopersicum*) cultivar MoneyMaker plants were root inoculated with *V. dahliae*, and plants were harvested at regular intervals from 4 to 16 days post-inoculation (dpi). After RNA isolation and cDNA synthesis, real-time polymerase chain reaction was performed to determine the relative expression levels of *VdNRS/ER* using the *V. dahliae* elongation factor 1-α gene as a reference. Expression at 4 dpi is set to unity.

plants (Fig. 4A). The absence of tomato colonization by *VdNRS/ER* deletion strains was confirmed by real-time PCR quantification of the fungal biomass (Fig. 5B). Importantly, pathogenicity was restored on complementation of the *VdNRS/ER* deletion strains with a genomic construct containing the wild-type *VdNRS/ER* locus (Fig. S2, see Supporting Information). Thus, it can be concluded that *VdNRS/ER* is required for pathogenicity on tomato. Collectively, our findings thus suggest that the T-DNA insertion 56 bp upstream of VDAG_06010 in random mutant 389 impaired the function of this gene, probably by impairing its expression *in planta*. However, as this mutant was no longer able to colonize tomato plants, the absence of gene expression during attempted host colonization could not be assessed.

To investigate whether the observed role of *VdNRS/ER* in pathogenicity is confined to tomato only, or also extends to other host species, we tested the pathogenicity of the *VdNRS/ER* deletion strains on the solanaceous model plant *N. benthamiana*. Similar to tomato, targeted deletion of *VdNRS/ER* resulted in compromised pathogenicity, as these plants remained devoid of *Verticillium* wilt symptoms (Fig. 4B). Again, loss of pathogenicity was confirmed by measurement of the canopy surface area (Fig. 5C) and by real-time PCR quantification of fungal biomass (Fig. 5D).

Absence of VdNRS/ER variation in a collection of *V. dahliae* strains

Allelic variation can be a sign of selection pressure and adaptation. To analyse potential VdNRS/ER diversity, we mined the genomes of 39 sequenced *V. dahliae* strains for the *VdNRS/ER* gene sequence (de Jonge *et al.*, 2012) (L. Faino and B. P. H. J. Thomma, unpublished data). Intriguingly, only two single nucleotide polymorphisms (SNPs) were identified in two strains, each at a different position and both resulting in a synonymous substitution that does not affect the sequence of the encoded protein. We thus conclude that these substitutions do not affect the function of VdNRS/ER.

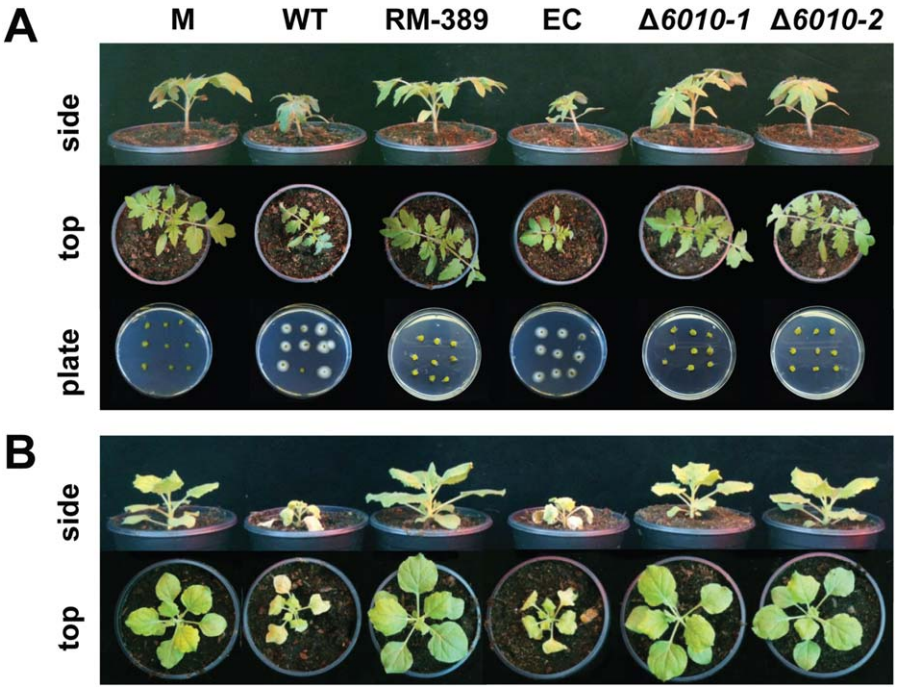

Fig. 4 *VdNRS/ER* (NRS/ER, nucleotide-rhamnose synthase/epimerase-reductase) is required for pathogenicity of *Verticillium dahliae* on tomato and *Nicotiana benthamiana*. (A) Top and side views of tomato cultivar MoneyMaker plants that were mock inoculated (M) or inoculated with wild-type *V. dahliae* (WT), random transformant RM-389, an ectopic transformant (EC) and two *VdNRS/ER* deletion strains (Δ*6010-1* and Δ*6010-2*) at 14 days post-inoculation (dpi). Fungal outgrowth at 7 days after plating of stem sections harvested at 14 dpi is shown at the bottom of the panel. (B) Top and side views of *N. benthamiana* plants inoculated as specified for (A).

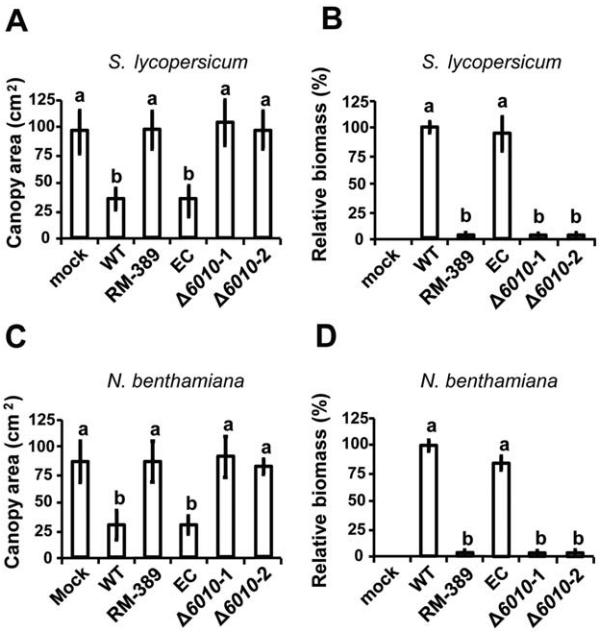

Fig. 5 *VdNRS/ER* (NRS/ER, nucleotide-rhamnose synthase/epimerase-reductase) is required for pathogenicity of *Verticillium dahliae* on tomato and *Nicotiana benthamiana*. Average canopy area of six tomato plants (A) and real-time polymerase chain reaction (PCR) quantification of fungal biomass (B) at 14 days after mock inoculation (mock) or inoculation with wild-type *Verticillium dahliae* (WT), random transformant (RM-389), an ectopic transformant (EC) and two *VdNRS/ER* deletion strains (Δ*6010-1* and Δ*6010-2*). Different letters indicate significant differences ($P < 0.05$). Average canopy area of six *N. benthamiana* plants (C) and real-time PCR quantification of fungal biomass (D) on inoculation as specified for (A) and (B).

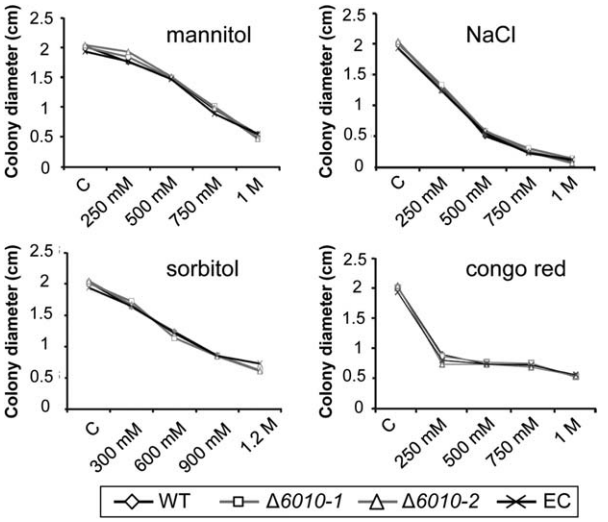

Fig. 6 Targeted deletion of *VdNRS/ER* (NRS/ER, nucleotide-rhamnose synthase/epimerase-reductase) does not affect cell wall integrity and osmotic stress resistance. Stress sensitivity assays were performed by placing a 5-μL droplet (10^6 conidia/mL) of wild-type *Verticillium dahliae* (WT), an ectopic transformant (EC) and two *VdNRS/ER* deletion strains (Δ*6010-1* and Δ*6010-2*) on Czapek-Dox medium (C) or Czapek-Dox medium supplemented with Congo red (250 mM, 500 mM, 750 mM and 1 M), NaCl (250 mM, 500 mM, 750 mM and 1 M), mannitol (250 mM, 500 mM, 750 mM and 1 M) or sorbitol (300 mM, 600 mM, 900 mM and 1.2 M). The colony diameter was measured after 7 days of incubation at 22°C.

VdNRS/ER is not required for cell wall integrity and osmotic stress resistance

To examine the role of *VdNRS/ER* in cell wall integrity and osmotic stress resistance, the random mutant (RM-389), *VdNRS/ER* deletion strains and ectopic transformant were grown on minimal agar medium supplemented with mannitol, sodium chloride, sorbitol or Congo red. After 7 days of growth, the colony diameter was measured, showing that mutant and wild-type strains were equally sensitive to the cell wall stress reagents (Fig. 6). These findings suggest that *VdNRS/ER* is not involved in cell wall integrity or osmotic stress resistance during mycelium development.

VdNRS/ER is required for tomato root colonization

To examine the role of *VdNRS/ER* in the initial stages of *V. dahliae* infection, the roots of 10-day-old tomato plants grown in a hydroponic solution were inoculated with conidiospores of the random mutant (RM-389), the *VdNRS/ER* deletion strains and the ectopic transformant. After 5 days of incubation, the tomato roots were inspected using a binocular microscope. Our data show that wild-type spores efficiently attached to the root surface, resulting in extensive fungal growth on the tomato roots (Fig. 7A). In contrast, little fungal growth was observed on roots inoculated with the random mutant (RM-389) or the *VdNRS/ER* deletion strains (Fig. 7A). The reduced fungal biomass of the random mutant (RM-389) and the *VdNRS/ER* deletion strains on the tomato roots was confirmed by quantitative PCR (Fig. 7B). Collectively, these data show that *VdNRS/ER* functions to contribute to successful colonization of roots by *V. dahliae*, potentially through root attachment.

VdNRS/ER is a functional enzyme that converts uridine diphosphate-4-keto-6-deoxy-glucose (UDP-KDG) to UDP-rhamnose

To examine whether *VdNRS/ER* is involved in the biosynthesis of UDP-rhamnose and to determine whether this activated sugar is the precursor for the synthesis of rhamnose-containing glycan, we examined the polysaccharide composition of *V. dahliae* grown *in vitro*. As mentioned previously, *VdNRS/ER* is expressed under various *in vitro* conditions. Thus, polysaccharides were extracted from conidiospores of wild-type *V. dahliae*, the *VdNRS/ER* deletion strain and the complementation strain, and analysed by gas chromatography-mass spectrometry (GC-MS). In the samples derived from wild-type *V. dahliae* and the complementation strain, a peak was detected that corresponds to rhamnose, which was

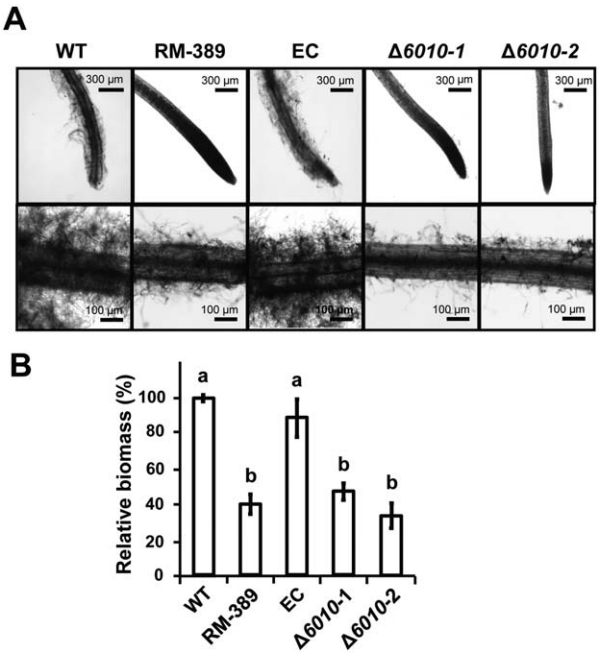

Fig. 7 *VdNRS/ER* (NRS/ER, nucleotide-rhamnose synthase/epimerase-reductase) is required for the colonization of tomato roots. Roots of 10-day-old tomato cultivar MoneyMaker seedlings were immersed in one-fifth potato dextrose broth (PDB) containing 10^6 conidia/mL of wild-type *Verticillium dahliae* (WT), random transformant (RM-389), an ectopic transformant (EC) and two *VdNRS/ER* deletion strains (Δ*6010-1* and Δ*6010-2*) for 72–96 h. (A) Roots were rinsed with water and photographed under a microscope. (B) Real-time polymerase chain reaction quantification of fungal biomass on the roots. Different letters indicate significant differences ($P < 0.05$).

absent in the *VdNRS/ER* deletion strain (Fig. 8). This finding confirms that *VdNRS/ER* is involved in rhamnose biosynthesis.

If rhamnose-containing glycans play a role during the early stages of host colonization, such as the attachment of conidiospores to the root, we anticipate that such glycans should be produced during conidiospore germination. Therefore, we determined the sugar composition of germinating conidiospores. Indeed, the sample derived from wild-type *V. dahliae* comprised a clear rhamnose peak (Fig. 9A,B) that was absent in samples from the *VdNRS/ER* deletion strain (Fig. 9C). Taken together, these results indicate that *VdNRS/ER* plays a role in the formation of rhamnose-containing glycan in germinating conidiospores during the early stages of host colonization.

In contrast with bacteria that produce dTDP-rhamnose in a three-step pathway, plants follow a two-step pathway to synthesize UDP-rhamnose (Oka *et al.*, 2007; Watt *et al.*, 2004). The genes involved in UDP-rhamnose production have also been identified recently in other fungi, including the rice pathogen *Magnaporthe oryzae* and the broad-host-range pathogen *Botrytis cinerea* (Martinez *et al.*, 2012). In *B. cinerea*, UDP-glucose is converted by a 4,6-dehydratase (BfDh) into an intermediate UDP-KDG that is subsequently converted by a bifunctional 3,5-epimerase/4-reductase (BfER, i.e. NRS/ER) into UDP-rhamnose (Martinez *et al.*, 2012). Thus, we examined whether VdNRS/ER, like BfER, is a functional enzyme that can convert UDP-KDG to UDP-rhamnose. To this end, the dual enzyme activities of recombinant VdNRS/ER and BfDh were analysed by liquid chromatography-mass spectrometry (LC-MS) using UDP-glucose (UDP-Glc) as a substrate (Martinez *et al.*, 2012). The first enzyme in the pathway is capable of converting UDP-Glc to UDP-KDG (Fig. 10B,D), as expected, and, with the addition of NRS/ER activity (VdNRS/ER), UDP-KDG was converted to UDP-rhamnose (Fig. 10C). The authenticity of UDP-rhamnose was determined by its elution and by its mass and MS/MS ion fragmentation (see inset in Fig. 10C). The enzyme activity of recombinant VdNRS/ER unambiguously shows that VdNRS/ER is a bifunctional enzyme with 3,5-epimerase and 4-reductase activities (Fig. 10E). Thus, we conclude that deletion of *VdNRS/ER* contributed to the loss of UDP-rhamnose formation and the lack of rhamnose-containing glycans during spore germination and the early stages of infection.

DISCUSSION

Rhamnose is found in a variety of fungal glycoproteins and exopolysaccharides, such as rhamnomannans. In our study, on a random mutant library generated in the vascular wilt fungus *V. dahliae*, we show, for the first time, that rhamnose-containing macromolecules are required for fungal pathogenicity through their contribution to the colonization of tomato roots. In random mutant 389, the T-DNA was integrated 56 bp upstream of the coding region of a putative NRS/ER. Our biochemical analyses of cell wall polysaccharides (Figs 8 and 9) and enzyme activity (Fig. 10C) confirm that VdNRS/ER is involved in UDP-rhamnose biosynthesis and show that this activated sugar is the precursor for rhamnose-containing glycan.

VdNRS/ER shows similarity to the bacterial rmlD substrate-binding domain, which is involved in the biosynthesis of dTDP-rhamnose. In Gram-negative bacteria, such as *Salmonella enterica*, *Vibrio cholerae* or *Escherichia coli*, L-rhamnose is an important residue in the O-antigen of lipopolysaccharides, which are essential for serum resistance and intestinal colonization (Chiang and Mekalanos, 1999). In mycobacteria, such as *Mycobacterium tuberculosis*, L-rhamnose maintains the structural integrity of the cell wall through connection of the inner peptidoglycan layer to the arabinogalactan polysaccharides (Giraud *et al.*, 2000). Moreover, disruption of dTDP-rhamnose biosynthesis in the plant growth-promoting rhizobacteria *Azospirillum brasilense* and *Azorhizobium caulinodans* results in reduced root attachment and colonization (Gao *et al.*, 2001; Jofré *et al.*, 2004). Furthermore, work on the foliar pathogen *Colletotrichum graminicola*, the causal agent of stalk rot of cereals and anthracnose of maize, has revealed the secretion of mucilaginous matrix by the fungus to promote the

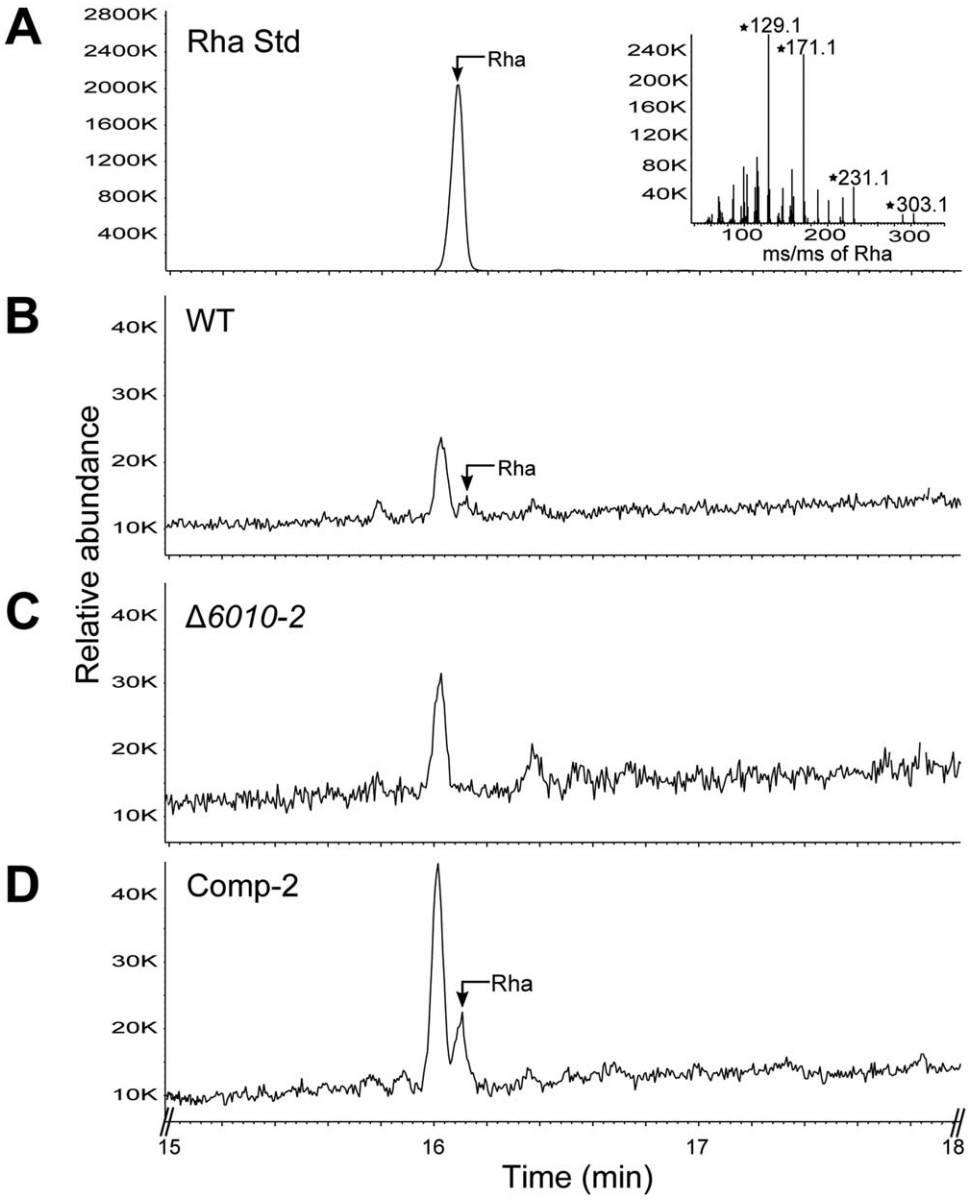

Fig. 8 *VdNRS/ER* (NRS/ER, nucleotide-rhamnose synthase/epimerase-reductase) deletion strains are depleted in uridine diphosphate (UDP)-rhamnose. Gas chromatography-mass spectrometry (GC-MS) analysis of alditol acetate derivatives of the glycosyl residues from conidiospore polysaccharides. (A) Total ion count chromatogram of alditol acetate-derived standard rhamnose (Rha) and mass spectrum (inset) showing fragmentation pattern fingerprints with *m/z* 129, 171, 231, 303. (B) Polysaccharides from wild-type *Verticillium dahliae* (WT) conidiospores display a peak eluting at 16.10 min that has the same retention time as rhamnose standard. (C) *VdNRS/ER* deletion strain (Δ*6010-1*) lacks a peak eluting at 16.10 min. (D) The *VdNRS/ER* deletion strain complemented with the native *VdNRS/ER* gene (Comp-2) displays a peak eluting at 16.10 min that has the same retention time as the rhamnose standard.

survival of fungal spores, the major component of which appeared to be high-molecular-weight glycoproteins containing rhamnose and mannose oligomers (Ramadoss *et al.*, 1985). Subsequently, this matrix was proposed to allow for the rapid adhesion of even ungerminated conidia to the hydrophobic plant surface to ensure germination and appressorium formation and the establishment of an infection court (Nicholson and Kunoh, 1995). Interestingly, further rhamnose-containing extracellular matrix is released on germ tube elongation to surround the hyphae and extend between them (Sugui *et al.*, 1999). Finally, a recent study has identified two genes encoding UDP-4,6-glucose dehydratase (UG4,6-Dh) and UDP-4-keto-6-deoxyglucose-3,5-epimerase-4-reductase (UDP4k6dG-ER) enzymes from *M. oryzae* and *B. cinerea* involved in UDP-rhamnose formation, although their contribution to pathogenicity was not investigated (Martinez *et al.*, 2012). Based on our study, however, strong evidence is presented that fungal UG4,6-Dh and U4k6dG-ER enzymes are involved in the formation of UDP-rhamnose, which is incorporated into rhamnose-containing polysaccharides that are crucial for fungal pathogenicity. Interestingly, the plant colonization-associated phenotypes observed thus far in our study and in those of others concern adhesion to various plant tissues, including roots, foliage and probably even the interior of xylem vessels, as *V. dahliae* is known to spread throughout the xylem by producing conidiospores that are carried with the water stream and that germinate once trapped, for instance at vessel ends (Fradin and Thomma, 2006). Arguably, the surfaces encountered under these conditions are highly divergent, for instance with respect to hydrophobicity, but

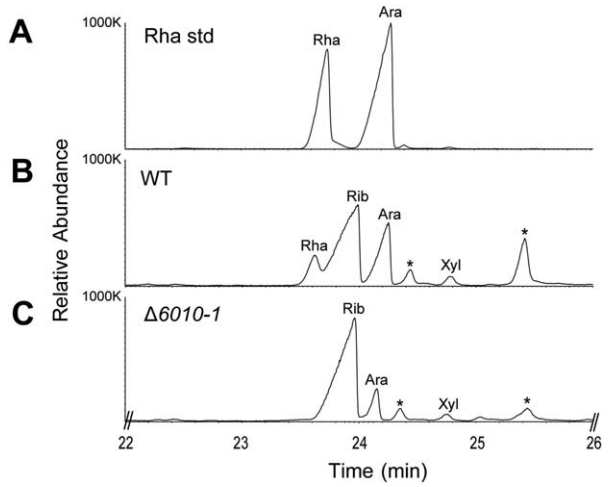

Fig. 9 Uridine diphosphate (UDP)-rhamnose is produced in germinating conidiospores. Gas chromatography-mass spectrometry (GC-MS) analysis of alditol acetate derivatives of the glycosyl residues from germinating conidiospore polysaccharides. (A) Total ion count chromatogram of alditol acetate-derived standard rhamnose (Rha). (B) Polysaccharides of conidiospores from wild-type *Verticillium dahliae* (WT) display a peak with the same retention time as the rhamnose standard. (C) *VdNRS/ER* (NRS/ER, nucleotide-rhamnose synthase/epimerase-reductase) deletion strain (*Δ6010-1*) does not display a rhamnose peak. Other peaks in the chromatogram correspond to ribose (Rib), arabinose (Ara) and xylose (Xyl). Asterisks indicate unidentified compounds that are not sugars.

also with respect to chemical composition. However, a full understanding of how rhamnose-containing macromolecules contribute to plant surface adhesion requires the identification of the rhamnose-containing macromolecules that are produced by the various plant-associated microbes, and their potential molecular targets in the various host plants.

Here, we have shown that targeted deletion of *VdNRS/ER* contributes to the loss of *V. dahliae* pathogenicity on various host plants. The role of rhamnose-containing macromolecules in cell wall integrity and oxidative stress tolerance in fungi is largely unknown. *VdNRS/ER* deletion strains were able to grow and sporulate without any visible defects, suggesting that rhamnose-containing glycans, such as glycoproteins, polysaccharides or exopolysaccharides, are not essential for vegetative growth or sporulation despite the observation that *VdNRS/ER* is expressed on growth *in vitro*. In addition, the growth rate of *VdNRS/ER* knockout mutants was not affected in the presence of inducers of cell wall stress and osmotic stress, suggesting that the rhamnose-containing glycans are not involved in functional cell wall structure and osmotic stress tolerance.

Based on the findings reported in this study, we propose a model to explain the contribution of UDP-rhamnose to the virulence of *V. dahliae* during infection on host plants. In the cytoplasm, UDP-glucose is converted into UDP-rhamnose in two steps using VdUG4,6-Dh and VdNRS/ER. The rhamnose of UDP-rhamnose is then transferred to glycan(s). The nature of these glycans remains unknown, but they consist of NaOH-solubilized cell wall polysaccharides and, potentially, glycoproteins. Presently, we cannot exclude the possibility that the rhamnose-containing polysaccharide is not an extracellular polysaccharide (EPS), as shown to be the case in *B. cinerea*. We propose that the rhamnose-containing glycan, produced during spore germination, plays a role in the attachment of spores to the root surface, which results in successful colonization of host plants. During host colonization, conidiospores are produced by *V. dahliae* in the xylem to facilitate the spread of the fungus throughout the host plant (Fradin and Thomma, 2006). Arguably, rhamnose then acts to facilitate conidiospore attachment to vessel ends and vessel walls in order to facilitate penetration into the next vessel elements. Thus, the production of conidiospores and subsequent germination is an ongoing process in repetitive cycles during disease progression, requiring continuous rhamnose biosynthesis. As *VdNRS/ER* deletion strains are unable to synthesize UDP-rhamnose and unable to cause disease, inhibitors of UDP-rhamnose synthesis may result in impaired pathogenicity and could present a novel strategy for disease control.

EXPERIMENTAL PROCEDURES

Agrobacterium tumefaciens-mediated transformation (ATMT)

The binary vector (pBHt2) harbouring the hygromycin B resistance gene (*hph*) under the control of the *Aspergillus nidulans trpC* promoter was used for ATMT (Mullins *et al.*, 2001). This vector was introduced to *A. tumefaciens* strain SK1044 to transform conidia of race 1 *V. dahliae* strain JR2, as described previously (Faino *et al.*, 2015; Santhanam, 2012). Briefly, *A. tumefaciens* was grown at 28 °C for 2 days in minimal medium supplemented with kanamycin (25 μg/mL). The *A. tumefaciens* cells were diluted to an optical density at 600 nm (OD_{600}) of 0.15 in induction medium (IM), supplemented with 200 μM acetosyringone (AS). The cells were grown for an additional 6 h before mixing them with an equal volume of *V. dahliae* conidiospore suspension (10^6 conidia/mL); 200 μL of this mixture was plated onto a Hybond-N^+ filter placed on IM supplemented with 200 μM AS. The plates were incubated in the dark at room temperature for 48 h after which the filter was transferred onto a selection plate [potato dextrose agar (PDA) supplemented with 50 μg/mL of hygromycin B and 200 μM of cefotaxime]. After 10–14 days, individual transformants were transferred to 24-well culture plates containing 1 mL of selection medium and incubated for 7–10 days. Spores from these cultures were stored in 30% glycerol at −80 °C until further analysis.

Plant inoculations

Pathogenicity assays were performed as described previously (Santhanam and Thomma, 2013). Briefly, individual transformants were subcultured in six-well culture plates for 7–10 days. Subsequently, 10 glass beads (~3 mm) and 3 mL of tap water were added to each of the wells and the plates were sealed. The conidiospores were released by shaking the plates for 15 min at 200 rpm on a reciprocal shaker, after which the sealant was

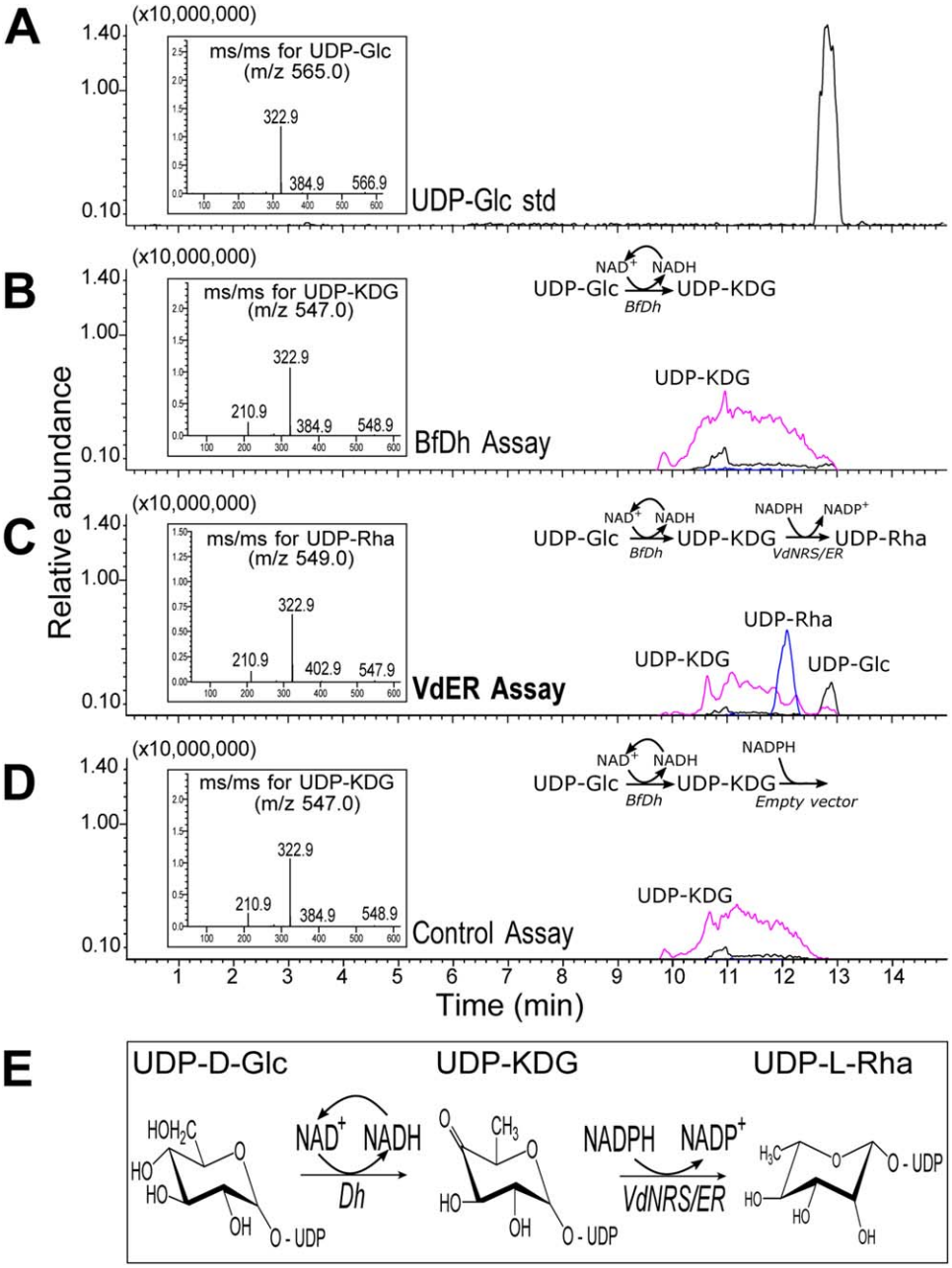

Fig. 10 VdNRS/ER (NRS/ER, nucleotide-rhamnose synthase/epimerase-reductase) converts uridine diphosphate-4-keto-6-deoxy-glucose (UDP-KDG) to UDP-rhamnose. (A) UDP-glucose (UDP-Glc) standard elutes from a HILIC (hydrophilic interaction liquid chromatography) column at 12.8 min and is detected by mass spectrometry (MS) with *m/z* 565 $[M - H]^-$. The MS/MS of the parent ion (inset) gives *m/z* 323 and 385 diagnostic ion fragments, $[UMP - H]^-$ and $[UDP - H_2O - H]^-$, respectively. (B) HILIC separation of products from the enzymatic reaction with BfDh (4,6-dehydratase) displays a peak with the same retention time as UDP-KDG with diagnostic $[M - H]^-$ *m/z* 547 and MS/MS ion fragment with *m/z* 323. (C) HILIC separation of products from the dual enzymatic reaction with BfDh and VdNRS/ER displays a peak with the same retention time as UDP-rhamnose (UDP-Rha) with diagnostic $[M - H]^-$ *m/z* 549 and MS/MS of 403, 323, 210. (D) Dual enzymatic reaction with BfDh and an empty vector control displays a peak with the same retention time as UDP-KDG with diagnostic $[M - H]^-$ *m/z* 547 and MS/MS ion fragment with *m/z* 323. (E) UDP-rhamnose metabolic pathway in fungi showing the enzymes involved in the sequential conversion of UDP-Glc to UDP-Rha.

removed. The roots of 10-day-old tomato (*Solanum lycopersicum* cv. MoneyMaker) seedlings were rinsed in water and dipped into the conidiospore suspension for 5 min. Seedlings were replanted in soil and scored for symptom development (wilting and stunting) up to 14 days. Seedlings that exhibited reduced *Verticillium* wilt symptoms when compared with wild-type *V. dahliae*-inoculated plants were identified and the corresponding mutants were retained for rescreening.

During rescreening, the infection assay was carried out essentially as described above, with the modification that the conidiospore concentration of the transformants was calibrated to 10^6 conidiospores/mL. The rescreening was repeated at least twice for each of the mutants that were retained in the initial screen.

Identification of T-DNA insertion sites

Genomic sequences flanking the T-DNA were isolated from the selected transformants with iPCR, as described previously (Meng *et al.*, 2007; Santhanam, 2012). Essentially, 500 ng of genomic DNA were digested overnight with *Msp*I or *Nco*I and heat-inactivated at 65 °C for 20 min. Subsequently, 50 μL of ligation mix (10 μL of 10 × T4 DNA ligase buffer, 5 units of T4 DNA ligase and 38 μL of H_2O) were added and incubated overnight at 15 °C. Next, the DNA was precipitated and dissolved in 50 μL of demineralized water. The genomic region flanking the T-DNA was amplified in 50 μL of reaction mix using 2 μL of ligation product, 1 μL of each primer (Table S1, see Supporting Information), 1 × PCR buffer,

0.6 μL of deoxynucleoside triphosphate (dNTP) mix (10 mM), 0.8 units of GO Taq DNA polymerase and 35.25 μL of water. The cycling conditions consisted of one cycle for 2 min at 94 °C, 35 cycles of 30 s at 94 °C, 30 s at 55 °C and 3 min at 72 °C, and a final extension step for 10 min at 72 °C. PCR products were purified and sequenced. The sequences obtained were used as query to BLAST against the *V. dahliae* genome (http://fungi.ensembl.org/Verticillium_dahliaejr2/Info/Index) (Faino *et al.*, 2015).

Targeted mutagenesis and complementation

To generate a *VdNRS/ER* deletion construct, sequences flanking the *VdNRS/ER* CDS were amplified from genomic DNA of *V. dahliae* strain JR2 using the primers KO-6010-LF with KO-6010-LR to amplify the left border, and KO-6010-RF with KO-6010-RR to amplify the right border, respectively (Table S1). The resulting amplicons were cloned into pRF-HU2 as described previously (Frandsen *et al.*, 2008). ATMT of *V. dahliae* was performed as described previously (Santhanam, 2012), and transformants were selected on PDA supplemented with 200 μg/mL of cefotaxime (Duchefa, Haarlem, the Netherlands) and 50 μg/mL of hygromycin (Duchefa). Homologous recombination was verified by PCR.

To generate a *VdNRS/ER* complementation construct, a 2404-bp *EcoR*I/*Pac*I fragment containing the VDAG_06010 (VDAG_JR2_Chr7g02960) CDS, with 1000-bp upstream and 450-bp downstream sequences, was amplified from *V. dahliae* strain JR2 genomic DNA, and cloned into binary vector pBT081 (Houterman *et al.*, 2008). Complementation transformants were selected on PDA supplemented with 200 μg/mL of cefotaxime and 100 μg/mL of phleomycin (InvivoGen, San Diego, CA, USA).

Growth, conidiogenesis and stress assays

Radial growth was monitored by placing a 2-μL droplet of a conidial suspension of 10^6 conidiospores/mL in the centre of PDA or Czapek-Dox medium, incubated at 22 °C and the colony diameter was measured after 10 days. For the quantification of conidiospore production, 5 mL of water were added to the culture and a conidial suspension was prepared by gently rubbing the mycelium. A 10-fold dilution of the conidial suspension was counted using a haemocytometer. Stress sensitivity assays were performed by placing a 2-μL droplet with 10^6 conidiospores/mL of wild-type *V. dahliae*, two *VdNRS/ER* deletion strains and an ectopic transformant in the centre of a Czapek-Dox plate supplemented with Congo red (250 mM, 500 mM, 750 mM and 1 M), NaCl (250 mM, 500 mM, 750 mM and 1 M), mannitol (250 mM, 500 mM, 750 mM and 1 M) or sorbitol (300 mM, 600 mM, 900 mM and 1.2 M), and incubated at 22 °C. Plates were photographed at 7 dpi and the colony diameter was measured using ImageJ software.

Root colonization assay

The root colonization assay was performed as described previously (Di Pietro *et al.*, 2001). Briefly, the roots of 10-day-old tomato seedlings were rinsed in water and placed in Erlenmeyer flasks containing a suspension of 10^6 conidia/mL in one-fifth potato dextrose broth (PDB), and incubated at 22 °C and 100 rpm. Fungal colonization of the root surface was observed macroscopically from 3 to 5 dpi. The experiments were performed three times with similar results.

Expression of recombinant VdNRS/ER

The following expression constructs were expressed in *E. coli* strain Bl21(DE3): pET-6hSUMO-VDAG_06010, containing a 6-histidine-small ubiquitin-like modifier (6hSUMO) tag fused to the N-terminus of *V. dahliae VdNRS/ER* (VDAG_06010); pET-6hSUMO was used as an empty vector control (pET-SUMO); pET28-BfDH4.1 (Martinez *et al.*, 2012) was used to express and purify the 6-histidine-tagged *Botryotinia fuckeliana* UDP-Glc 4,6-dehydratase (BfDH). The *E. coli* strains carrying the different constructs were cultured for 16 h at 37 °C in LB medium supplemented with 50 μg/mL kanamycin and 35 μg/mL chloramphenicol. On the following day, 5-mL cultures were transferred to 245 mL of fresh LB liquid medium supplemented with the same antibiotics, and cell growth was resumed at 37 °C at 220 rpm until the cell density reached an OD_{600} of ~0.6. Gene expression was then induced by the addition of isopropyl β-D-thiogalactoside (0.5 mM), and cultures were grown for an additional 20 h at 18 °C at 220 rpm. Cells were collected by centrifugation (6000 ***g*** for 10 min at 4 °C) and suspended in 10 mL of lysis buffer [50 mM Tris-HCl, pH 7.5, 10% glycerol, 1 mM ethylenediaminetetraacetic acid (EDTA), 2 mM dithiothreitol (DTT), 0.5 mM phenylmethylsulfonylfluoride (PMSF), with or without 50 mM NaCl]. Cells were lysed in an ice bath with an S-4000 sonicator (Misonix Inc., Farmingdale, NY, USA) equipped with a 1/8-in microtip probe using 12 sonication cycles (10 s pulse; 20 s off). The lysed cells were centrifuged (6000 ***g*** for 10 min at 4 °C); the supernatant was supplemented with 1 mM DTT and centrifuged again (20 000 ***g*** for 30 min at 4 °C). The resulting supernatant was kept at −20 °C. Protein purification was carried out as described previously (Martinez *et al.*, 2012).

Enzyme assays

The dual activity of recombinant enzymes BfDH and *VdNRS/ER* was analysed by LC-MS in a total volume of 50 μL, containing 50 mM Tris-HCl, pH 6.5, 0.25 mM UDP-Glc, 0.5 mM NAD^+, 0.5 mM NADPH, 5 μL of purified *B. fuckeliana* BfDH with or without the addition of 2 μL of *VdNRS/ER*. The reaction was incubated at 37 °C for 1 h and terminated by heating for 5 min at 95 °C. After the addition of chloroform and centrifugation (10 000 ***g*** for 4 min), an aliquot (20 μL) of the upper phase layer was removed and mixed with 38 μL of acetonitrile and 2 μL of 0.5 M ammonium acetate, pH 4.35. A portion (25 μL) of this mixture was analysed using HILIC (hydrophilic interaction liquid chromatography) and mass spectrometry analyses. This was performed using an liquid chromatography- mass spectrometry electrospray ionization-ion trap-time of flight (LC-MS/MS IT-TOF MS) system (Shimadzu Scientific Instruments, Columbia, MD, USA) operating in the negative ion mode with a Nexera, Shimadzu, Columbia, MD, USA UFPLC LC-30AD pump (Shimadzu), autosampler (Sil30) and column heater (set to 37 °C). Nucleotide sugars were separated on an Accucore, Waltham, MA, USA 150-amide HILIC column (150 × 4.6 mm^2, 2.6 μm particle size, Thermo Scientific, Waltham, MA, USA) using 40 mM ammonium acetate, pH 4.3 (solvent A), and acetonitrile (solvent B) with the gradient conditions as in Li *et al.* (2015).

Isolation of polysaccharide and sugar analyses by GC-MS

Conidiospores were harvested from 7-day-old *V. dahliae* cultures grown on PDA (Thermo Fisher Scientific Inc., Breda, the Netherlands).

Germinating spores were prepared by inoculating 30 μL of conidiospores into 12.5 mL of Gamborg's Glc (2%) on a medium-sized plate (9 cm). The plates were incubated for 66 h at room temperature under regular light to allow the spores to germinate. Polysaccharides were either extracted directly from conidospore samples or from germinating conidiospores (<100 μg) *s*tarting by incubation for 3 h at 80 °C whilst stirring with 5 mL of 1 M NaOH. After centrifugation (10 000 ***g***, 4 °C, 10 min), the alkaline extract was mixed with an equal volume of 96% ethanol. Following centrifugation (10 000 ***g***, 4 °C, 15 min), the pellet was resuspended in 10 mL of water and dialysed (3000 molecular weight cut-off) against two 10-L changes of deionized water. The dialysed solution was centrifuged (10 000 ***g***, 4 °C, 15 min) and the water-soluble supernatant alkaline water soluble (aWS) was collected and freeze–dried. The glycosyl residue compositions of these extracts were then determined.

An aliquot of each extract (1 mg) was supplemented with 10 μg inositol and hydrolysed with 1 mL of 2 M trifluoroacetic acid at 120 °C. The released monosaccharides were reduced to their alditols (York *et al.*, 1986) and acetylated. The resulting alditol acetate derivatives were analysed by a GC-MS system consisting of a gas chromatograph (Agilent 7890a; Agilent Technologies, Santa Clara, CA, USA) equipped with an EI-MS detector (5975c). A 1-μL sample or standard was injected via an Agilent 7693 autosampler injector port (Agilent Technologies) (set at 250 °C; 3 mL/min helium) in a split (1 : 50) mode into a non-polar Equity-1 capillary column (30 m × 0.25 mm i.d.; film thickness, 0.25 μm). The chromatography gas carrier was helium (1 mL/min) and the column oven temperature program used to separate the sugar derivatives was as follows: initial injection temperature of 60 °C for 1 min, followed by an increase of 27.5 °C/min to 170 °C, then of 4 °C/min to 235 °C, and a hold at 235 °C for 2 min. The column was then kept at 260 °C for 12 min, cooled to 60 °C and then kept at 60 °C for 1 min prior to the next sample injection. The temperature of the transfer line between the column ends to the mass spectrometer was 250 °C. Detection was achieved using EI-MS operating with an electron impact ionization energy of 70 V with the temperature of the MS ion source set at 230 °C and that of the quad at 150 °C. MS data were collected in full scan monitoring mode in the *m/z* range 50–550 from 5 to 50 min. The spectra were analysed using Software MSD ChemStation D.02.00.275 (Agilent Technologies). Alditol acetate derivatives of monosaccharide standards (50 μg each of rhamnose, fucose, xylose, mannose and glucose, and 30 μg each of ribose, arabinose and galactose), supplemented with 10 μg inositol (internal standard), were prepared under the same conditions as the samples. For data analysis, sugar residue peaks were identified based on the retention times of standard monosaccharides and their characteristic mass spectra.

ACKNOWLEDGEMENTS

B.P.H.J.T. was supported by a Vici grant from the Research Council for Earth and Life Sciences (ALW) of the Netherlands Organization for Scientific Research (NWO). This research was funded in part by Binational Agriculture Research and Development fund (BARD) grant # IS 4501-12 to M.B.P. The funders had no role in the study design, data collection and analysis, decision to publish, or preparation of the manuscript. The authors declare no conflicts of interest. The authors thank Hugo de Vries and Emilie Fradin for technical assistance, and Bert Essenstam and Henk Smid for excellent plant care.

REFERENCES

Bolek, Y., El-Zik, K.M., Pepper, A.E., Bell, A.A., Magill, C.W., Thaxton, P. M. and Reddy, O. U. K. (2005) Mapping of Verticillium wilt resistance genes in cotton. *Plant Sci.* **168**, 1581–1590.

Chiang, S.L. and Mekalanos, J.J. (1999) rfb mutations in *Vibrio cholerae* do not affect surface production of toxin-coregulated pili but still inhibit intestinal colonization. *Infect. Immun.* **67**, 976–980.

Di Pietro, A., Garcia-MacEira, F.I., Meglecz, E. and Roncero, M.I. (2001) A MAP kinase of the vascular wilt fungus *Fusarium oxysporum* is essential for root penetration and pathogenesis. *Mol. Microbiol.* **39**, 1140–1152.

Faino, L., de Jonge, R. and Thomma, B.P.H.J. (2012) The transcriptome of *Verticillium dahliae*-infected *Nicotiana benthamiana* determined by deep RNA sequencing. *Plant Signal. Behav.* **7**, 1065–1069.

Faino, L., Seidl, M.F., Datema, E., van den Berg, G.C., Janssen, A., Wittenberg, A. H. and Thomma, B. P. H. J. (2015) Single-molecule real-time sequencing combined with optical mapping yields completely finished fungal genome. *MBio*, **6**, e00936–15.

Fradin, E.F. and Thomma, B.P.H.J. (2006) Physiology and molecular aspects of Verticillium wilt diseases caused by *V. dahliae* and *V. albo-atrum*. *Mol. Plant Pathol.* **7**, 71–86.

Fradin, E.F., Zhang, Z., Juarez Ayala, J.C., Castroverde, C.D., Nazar, R.N., Robb, J., Liu, C. M. and Thomma, B. P. H. J. (2009) Genetic dissection of Verticillium wilt resistance mediated by tomato Ve1. *Plant Physiol.* **150**, 320–332.

Frandsen, R.J., Andersson, J.A., Kristensen, M.B. and Giese, H. (2008) Efficient four fragment cloning for the construction of vectors for targeted gene replacement in filamentous fungi. *BMC Mol. Biol.* **9**, 70.

Gao, M., D'Haeze, W., De Rycke, R., Wolucka, B. and Holsters, M. (2001) Knockout of an azorhizobial dTDP-L-rhamnose synthase affects lipopolysaccharide and extracellular polysaccharide production and disables symbiosis with *Sesbania rostrata*. *Mol. Plant–Microbe Interact.* **14**, 857–866.

Giesbert, S., Schumacher, J., Kupas, V., Espino, J., Segmuller, N., Haeuser-Hahn, I., Schreier, P. H. and Tudzynski, P. (2012) Identification of pathogenesis-associated genes by T-DNA-mediated insertional mutagenesis in *Botrytis cinerea*: a type 2A phosphoprotein phosphatase and an SPT3 transcription factor have significant impact on virulence. *Mol. Plant–Microbe Interact.* **25**, 481–495.

Giraud, M.F., Leonard, G.A., Field, R.A., Berlind, C. and Naismith, J.H. (2000) RmlC, the third enzyme of dTDP-L-rhamnose pathway, is a new class of epimerase. *Nat. Struct. Mol. Biol.* **7**, 398–402.

Hayes, R.J., McHale, L.K., Vallad, G.E., Truco, M.J., Michelmore, R.W., Klosterman, S. J., Maruthachalam, K. and Subbarao, K. V. (2011) The inheritance of resistance to Verticillium wilt caused by race 1 isolates of *Verticillium dahliae* in the lettuce cultivar La Brillante. *Theor. Appl. Genet.* **123**, 509–517.

Houterman, P.M., Cornelissen, B.J. and Rep, M. (2008) Suppression of plant resistance gene-based immunity by a fungal effector. *PLoS Pathog.* **4**, e1000061.

Hüser, A., Takahara, H., Schmalenbach, W. and O'Connell, R. (2009) Discovery of pathogenicity genes in the crucifer anthracnose fungus *Colletotrichum higginsianum*, using random insertional mutagenesis. *Mol. Plant–Microbe Interact.* **22**, 143–156.

Jeon, J., Park, S.Y., Chi, M.H., Choi, J., Park, J., Rho, H. S., Kim, S., Goh, J., Yoo, S., Choi, J., Park, J. Y., Yi, M., Yang, S., Kwon, M. J., Han, S. S., Kim, B. R., Khang, C. H., Park, B., Lim, S. E., Jung, K., Kong, S., Karunakaran, M., Oh, H. S., Kim, H., Kim, S., Park, J., Kang, S., Choi, W. B., Kang, S. and Lee, Y. H. (2007) Genome-wide functional analysis of pathogenicity genes in the rice blast fungus. *Nat. Genet.* **39**, 561–565.

Jofré, E., Lagares, A. and Mori, G. (2004) Disruption of dTDP-rhamnose biosynthesis modifies lipopolysaccharide core, exopolysaccharide production, and root colonization in *Azospirillum brasilense*. *FEMS Microbiol. Lett.* **231**, 267–275.

de Jonge, R., van Esse, H.P., Maruthachalam, K., Bolton, M.D., Santhanam, P., Saber, M. K., Zhang, Z., Usami, T., Lievens, B., Subbarao, K. V. and Thomma, B. P. H. J. (2012) Tomato immune receptor Ve1 recognizes effector of multiple fungal pathogens uncovered by genome and RNA sequencing. *Proc. Natl. Acad. Sci. USA*, **109**, 5110–5115.

de Jonge, R., Bolton, M.D., Kombrink, A., van den Berg, G.C., Yadeta, K.A. and Thomma, B. P. H. J. (2013) Extensive chromosomal reshuffling drives evolution of virulence in an asexual pathogen. *Genome Res.* **23**, 1271–1282.

Klimes, A., Dobinson, K.F., Klosterman, S.J. and Thomma, B.P.H.J. (2015) Genomics spurs rapid advances in our understanding of the basic biology of vascular wilt pathogens in the genus Verticillium. *Annu. Rev. Phytopathol.* **53**, 181–198.

Klosterman, S.J., Atallah, Z.K., Vallad, G.E. and Subbarao, K.V. (2009) Diversity, pathogenicity, and management of Verticillium species. *Annu. Rev. Phytopathol.* **47**, 39–62.

Klosterman, S. J., Subbarao, K. V., Kang, S., Veronese, P., Gold, S. E., Thomma, B. P. H. J., Chen, Z., Henrissat, B., Lee, Y. H., Park, J., Garcia-Pedrajas, M. D., Barbara, D. J., Anchieta, A., de Jonge, R., Santhanam, P., Maruthachalam, K., Atallah, Z., Amyotte, S. G., Paz, Z., Inderbitzin, P., Hayes, R. J., Heiman, D. I., Young, S., Zeng, Q., Engels, R., Galagan, J., Cuomo, C. A., Dobinson, K. F. and Ma, L. J. (2011) Comparative genomics yields insights into niche adaptation of plant vascular wilt pathogens. *PLoS Pathog.* **7**, e1002137.

Korn, M., Schmidpeter, J., Dahl, M., Muller, S., Voll, L. M. and Koch, C. (2015) A genetic screen for pathogenicity genes in the hemibiotrophic fungus *Colletotrichum higginsianum* identifies the plasma membrane proton pump pma2 required for host penetration. *PLoS One*, **10**, e0125960.

Li, Z., Hwang, S., Ericson, J., Bowler, K. and Bar-Peled, M. (2015) Pen and Pal are nucleotide-sugar dehydratases that convert UDP-GlcNac to UDP-6-deoxy-D-GlcNac-5,6-ene and then to UDP-4-keto-6-deoxy-L-AltNac for CMP-Pseudaminic acid synthesis in *Bacillus thuringiensis*. *J. Biol. Chem.* **290**, 691–704.

Martinez, V., Ingwers, M., Smith, J., Glushka, J., Yang, T. and Bar-Peled, M. (2012) Biosynthesis of UDP-4-keto-6-deoxyglucose and UDP-rhamnose in pathogenic fungi *Magnaporthe grisea* and *Botryotinia fuckeliana*. *J. Biol. Chem.* **287**, 879–892.

Maruthachalam, K., Klosterman, S.J., Kang, S., Hayes, R.J. and Subbarao, K.V. (2011) Identification of pathogenicity-related genes in the vascular wilt fungus *Verticillium dahliae* by *Agrobacterium tumefaciens*-mediated T-DNA insertional mutagenesis. *Mol. Biotechnol.* **49**, 209–221.

Meng, Y., Patel, G., Heist, M., Betts, M. F., Tucker, S. L., Galadima, N., Donofrio, N. M., Brown, D., Mitchell, T. K., Li, L., Xu, J. R., Orbach, M., Thon, M., Dean, R. A. and Farman, M. L. (2007) A systematic analysis of T-DNA insertion events in *Magnaporthe oryzae*. *Fungal Genet. Biol.* **44**, 1050–1064.

Michielse, C.B., van Wijk, R., Reijnen, L., Cornelissen, B.J. and Rep, M. (2009) Insight into the molecular requirements for pathogenicity of *Fusarium oxysporum* f. sp. *lycopersici* through large-scale insertional mutagenesis. *Genome Biol.* **10**, R4.

Mullins, E., Chen, X., Romaine, P., Raina, R., Geiser, D. and Kang, S. (2001) Agrobacterium-mediated transformation of *Fusarium oxysporum*: an efficient tool for insertional mutagenesis and gene transfer. *Phytopathology*, **91**, 173–180.

Munch, S., Ludwig, N., Floss, D. S., Sugui, J. A., Koszucka, A. M., Voll, L. M., Sonnewald, U. and Deising, H. B. (2011) Identification of virulence genes in the corn pathogen *Colletotrichum graminicola* by *Agrobacterium tumefaciens*-mediated transformation. *Mol. Plant Pathol.* **12**, 43–55.

Nicholson, R.L. and Kunoh, H. (1995) Early interactions, adhesion, and establishment of the infection court by *Erysiphe graminis*. *Can. J. Bot.* **73**, 609–615.

Oka, T., Nemoto, T. and Jigami, Y. (2007) Functional analysis of Arabidopsis thaliana RHM2/MUM4, a multidomain protein involved in UDP-D-glucose to UDP-L-rhamnose conversion. *J. Biol. Chem.* **282**, 5389–5403.

Pegg, G.F. and Brady, B.L. (2002) *Verticillium Wilts*. CABI publishing, Wallingford, UK.

Ramadoss, C.S., Uhlig, J., Carbon, D.M., Butler, L.G. and Nicholson, R.L. (1985) Composition of the mucilaginous spore matrix of *Colletotrichum graminicola*, a pathogen of corn, sorghum, and other grasses. *J. Agric. Food Chem.* **33**, 728–732.

Ramos, B., Gonzalez-Melendi, P., Sanchez-Vallet, A., Sanchez-Rodriguez, C., Lopez, G. and Molina, A. (2013) Functional genomics tools to decipher the pathogenicity mechanisms of the necrotrophic fungus *Plectosphaerella cucumerina* in *Arabidopsis thaliana*. *Mol. Plant Pathol.* **14**, 44–57.

Rowe, R.C., Davis, J.R., Powelson, M.L. and Rouse, D.I. (1987) Potato early dying: causal agents and management strategies. *Plant Dis.* **71**, 482–489.

Santhanam, P. (2012) Random insertional mutagenesis in fungal genomes to identify virulence factors. In: *Plant fungal pathogens. Methods in molecular biology*, (Bolton MD, T. B., ed.). Totowa: Humana press, pp. 509–517.

Santhanam, P. and Thomma, B.P.H.J. (2013) *Verticillium dahliae* Sge1 differentially regulates expression of candidate effector genes. *Mol. Plant–Microbe Interact.* **26**, 249–256.

Santhanam, P., van Esse, H. P., Albert, I., Faino, L., Nurnberger, T. and Thomma, B. P. H. J. (2013) Evidence for functional diversification within a fungal NEP1-like protein family. *Mol. Plant–Microbe Interact.* **26**, 278–286.

Schaible, L., Cannon, O.S. and Waddoups, V. (1951) Inheritance of resistance to Verticillium wilt in a tomato cross. *Phytopathology*, **41**, 986–990.

Schumacher, J., Simon, A., Cohrs, K.C., Viaud, M. and Tudzynski, P. (2014) The transcription factor BcLTF1 regulates virulence and light responses in the necrotrophic plant pathogen *Botrytis cinerea*. *PLoS Genet.* **10**, e1004040.

Simko, I., Haynes, K. G., Ewing, E. E., Costanzo, S., Christ, B. J. and Jones, R. W. (2004) Mapping genes for resistance to *Verticillium albo-atrum* in tetraploid and diploid potato populations using haplotype association tests and genetic linkage analysis. *Mol. Genet. Genomics*, **271**, 522–531.

Singh, S., Braus-Stromeyer, S. A., Timpner, C., Tran, V. T., Lohaus, G., Reusche, M., Knufer, J., Teichmann, T., von Tiedemann, A. and Braus, G. H. (2010) Silencing of Vlaro2 for chorismate synthase revealed that the phytopathogen *Verticillium longisporum* induces the cross-pathway control in the xylem. *Appl. Microbiol. Biotechnol.* **85**, 1961–1976.

Sugui, J.A., Kunoh, H. and Nicholson, R.L. (1999) Detection of protein and carbohydrate in the extracellular matrix released by *Cochliobolus heterostrophus* during germination. *Mycoscience*, **40**, 11–19.

Thomma, B.P.H.J., Nurnberger, T. and Joosten, M.H.A.J. (2011) Of PAMPs and effectors: the blurred PTI–ETI dichotomy. *Plant Cell*, **23**, 4–15.

Timpner, C., Braus-Stromeyer, S.A., Tran, V.T. and Braus, G.H. (2013) The Cpc1 regulator of the cross-pathway control of amino acid biosynthesis is required for pathogenicity of the vascular pathogen *Verticillium longisporum*. *Mol. Plant–Microbe Interact.* **26**, 1312–1324.

Tzima, A.K., Paplomatas, E.J., Rauyaree, P., Ospina-Giraldo, M.D. and Kang, S. (2011) VdSNF1, the sucrose nonfermenting protein kinase gene of *Verticillium dahliae*, is required for virulence and expression of genes involved in cell-wall degradation. *Mol. Plant–Microbe Interact.* **24**, 129–142.

Watt, G., Leoff, C., Harper, A.D. and Bar-Peled, M. (2004) A bifunctional 3,5-epimerase/4-keto reductase for nucleotide-rhamnose synthesis in Arabidopsis. *Plant Physiol.* **134**, 1337–1346.

Wilhelm, S. (1955) Longevity of the Verticillium wilt fungus in the laboratory and field. *Phytopathology*, **45**, 180–181.

Winnenburg, R., Baldwin, T. K., Urban, M., Rawlings, C., Köhler, J. and Hammond-Kosack, K. E. (2006) PHI-base: a new database for pathogen host interactions. *Nucleic Acids Res.* **34**, D459–D464.

Winnenburg, R., Urban, M., Beacham, A., Baldwin, T. K., Holland, S., Lindeberg, M., Hansen, H., Rawlings, C., Hammond-Kosack, K. E. and Kohler, J. (2008) PHI-base update: additions to the pathogen host interaction database. *Nucleic Acids Res.* **36**, D572–D576.

Xu, L. and Chen, W. (2013) Random T-DNA mutagenesis identifies a Cu/Zn superoxide dismutase gene as a virulence factor of *Sclerotinia sclerotiorum*. *Mol. Plant–Microbe Interact.* **26**, 431–441.

York, W.S., Darvill, A.G., McNeil, M., Stevenson, T.T. and Albersheim, P. (1986) Isolation and characterization of plant cell walls and cell wall components. *Methods Enzymol.* **118**, 3–40.

SUPPORTING INFORMATION

Additional Supporting Information may be found in the online version of this article at the publisher's website:

Fig. S1 Verification of deletion and complementation strains by polymerase chain reaction (PCR). (A) Amplification of the T-DNA flanking sequences from wild-type *Verticillium dahliae* (w), 10 independent random transformants (lanes 1–10) and the marker (m). (B) Amplification of the hygromycin resistance gene (*hph*) and *VdNRS/ER* from 10 independent transformants (lanes 1–10) and wild-type *V. dahliae* (w). The marker (m) is indicated. True deletion strains are marked with asterisks, and the ectopic transformant is marked with an arrow. (C) Amplification of the zeocin resistance gene (*ble*) and *VdNRS/ER* from five independent complementation strains (lanes 1–5), a *VdNRS/ER* deletion strain (*) and wild-type *V. dahliae* (w). The marker (m) and true complementation strains (+) are indicated.

Fig. S2 Complementation of *VdNRS/ER* deletion strain restores pathogenicity on tomato. (A) Side and top views of tomato cultivar MoneyMaker plants inoculated with wild-type *Verticillium dahliae* (WT), a *VdNRS/ER* deletion strain (Δ*6010-1*) and two complementation strains (Comp-1 and Comp-2), or mock inoculated at 14 days post-inoculation (dpi). (B) Fungal outgrowth at 7 days after plating of stem sections harvested at 14 dpi. (C) Average canopy area of six plants at 14 dpi as described for (A). Different letters indicate significant differences ($P < 0.05$).
Table S1 Primers used in this study.